



Calculation of Duct Flow Noise Using CE/SE Method

Horus Y. H. CHAN¹; Garret C. Y. LAM²; Randolph C. K. LEUNG³

^{1,2,3} Department of Mechanical Engineering, The Hong Kong Polytechnic University, P. R. China

ABSTRACT

Noise generated in flow duct propagates extensively through the connected ductwork. Its propagation through the outlets would contribute to indoor acoustic discomfort and results in environmental problem. Silencers with acoustic lining are commonly adopted for noise mitigation in flow duct. Researchers have been devoting many numerical efforts in assessing the performance of a liner design. In general, numerical studies are performed by either time domain or frequency domain approach. This paper reports a development of calculation method solving Acoustic Perturbation Equations and Time-Domain Impedance Boundary on the Conservation Element and Solution Element (CE/SE) framework to calculate duct noise problem in time domain. In this paper, three benchmark cases are presented to verify the capability of the proposed method on calculating the flow induced acoustic generation, propagation, and the acoustic behavior at the impedance boundaries in the presence and absence of flow.

Keywords: Duct Noise, CE/SE, Liner I-INCE Classification of Subjects Number(s): 76.9
(See <http://www.inceusa.org/links/Subject%20Class%20-%20Formatted.pdf>.)

1. INTRODUCTION

With the development of engineering technology, noise problem has long been an awareness as a side product of various engineering systems, e.g. ventilation systems. The generated noise in these system is easily propagated through flow duct to occupancy zones causing discomfort to people and environmental problem. Silencers with acoustic lining are commonly installed between the noise sources and the occupancy zones so as to attenuate the noise level there. Acoustic lining is usually made of fiberglass or other porous materials for absorbing the noise. Since the design of silencer varies depending on operating condition, the investigation and optimization of acoustic performance are usually carried out numerically.

Generally, these numerical investigations are calculated by either time domain or frequency domain approach. Compared to the frequency domain method the time domain calculation method can account for the nonlinear effects and capture the transient effects, which make it popular in aeroacoustic study. One of the most popular technique assessing the liner behavior in aeroacoustic problem is to solve the perturbed equations using a hybrid calculation method. This method divides the aeroacoustic calculation into two steps. First, the near field flow dynamics is calculated by Computational Fluid Dynamics solver. Then the acoustic generation and propagation is calculated by solving the perturbed equations, e.g. Acoustic/Viscous Splitting Technique (1), Linearized Euler Equations (2), based on the calculated flow solution. Another improved formulation, Acoustic Perturbation Equations (APE), proposed by Ewert and Schröder (3) applies a source filter to suppress the calculation instability. Finally, the acoustic behavior of liner is modeled as a time domain impedance boundary condition in the acoustic solver, e.g. Ma and Zhang (4). Moreover, these techniques are usually highly computational demanding because they are developed on high order numerical schemes (at least 6th order).

In this paper, we propose a low order, yet accurate Space-Time Conservation Element and Solution Element (CE/SE) method to solve APE along with the implementation of time domain impedance boundary condition (TDIBC). The CE/SE method is adopted due to its simplicity, inexpensive but robust characteristics. This calculation method is assessed by several benchmark cases: acoustic generation by co-rotating vortex pair, acoustic pulse reflection in normal incidence tube and NASA grazing incidence tube. These can demonstrate the capability of the solver in capturing the acoustic generation, propagation, reflection from normal/grazing incidence impedance wall with and without flow.

¹yui.ho.chan.me@connect.polyu.hk

²garret.lam.hk@connect.polyu.hk

³mmrleung@polyu.edu.hk

The paper is organized as follows: in Section 2, the formulation of APE is introduced; in Section 3, the CE/SE method is briefly discussed; in Section 4, we present the time domain impedance boundary condition used in the calculation method; in Section 5, the result of three calculations are discussed and compared with analytical/experimental results; in Section 6, we present the conclusions.

2. ACOUSTIC PERTURBATION EQUATIONS

The first hybrid approach is the acoustic/viscous splitting method proposed by Hardin and Pope (1) in 1994. Other researchers (5, 6) have proposed modifications so as to reduce the growth of hydrodynamic instabilities. In the present work, a hybrid method based on solving the Acoustic Perturbation Equations (APE) (3) is adopted. A total quantity Φ can be decomposed into a fluctuating component Φ' and a time-averaged component $\bar{\Phi}$, i.e. $\Phi = \Phi' + \bar{\Phi}$. While the fluctuating component is further decomposed into vortical mode Φ'_v , entropy mode Φ'_e and acoustic mode Φ'_a . In APE, an acoustic filter is applied such that only acoustic mode fluctuation is generated by vortical source and heat source.

There are several variations of APE, but only the APE-4 system, is chosen due to its better accuracy. It can be written in a strong conservative form as,

$$\frac{\partial \mathbf{U}}{\partial t} + \frac{\partial \mathbf{F}}{\partial x} + \frac{\partial \mathbf{G}}{\partial y} = \mathbf{Q}, \quad (1)$$

$$\mathbf{U} = \left[p', u', v' \right]^T, \quad (2)$$

$$\mathbf{F} = \left[\bar{c}^2 \left(\bar{\rho} u' + \bar{u} \frac{p'}{\bar{c}^2} \right), \bar{u} \cdot u' + \frac{p'}{\bar{\rho}}, 0 \right]^T, \quad (3)$$

$$\mathbf{G} = \left[\bar{c}^2 \left(\bar{\rho} v' + \bar{v} \frac{p'}{\bar{c}^2} \right), 0, \bar{v} \cdot v' + \frac{p'}{\bar{\rho}} \right]^T, \quad (4)$$

$$\mathbf{Q} = \left[\begin{array}{c} - \left(\frac{\partial(\rho' u')}{\partial x} + \frac{\partial(\rho' v')}{\partial y} \right) + \frac{\bar{p}}{c_p} \frac{D s'}{D t} \\ (\boldsymbol{\omega} v)' + T' \frac{\partial \bar{s}}{\partial x} - \bar{T} \frac{\partial s'}{\partial x} - \left(\frac{\partial}{\partial x} \frac{(u')^2}{2} \right)' + \left(\frac{\partial}{\partial x} \cdot \frac{\boldsymbol{\tau}}{\bar{\rho}} \right)' \\ - (\boldsymbol{\omega} u)' + T' \frac{\partial \bar{s}}{\partial y} - \bar{T} \frac{\partial s'}{\partial y} - \left(\frac{\partial}{\partial y} \frac{(v')^2}{2} \right)' + \left(\frac{\partial}{\partial y} \cdot \frac{\boldsymbol{\tau}}{\bar{\rho}} \right)' \end{array} \right], \quad (5)$$

where ρ , $\mathbf{u} = (u, v)$, p , s , T , $\boldsymbol{\tau}$, $\boldsymbol{\omega} = \nabla \times \mathbf{u}$ are density, velocity, pressure, entropy, temperature, stress tensor and vorticity respectively. In the linear approximation, those small non-linear terms $\left(\frac{\partial(\rho' u')}{\partial x} + \frac{\partial(\rho' v')}{\partial y} \right)$, $\left(\frac{\partial}{\partial x} \frac{(u')^2}{2} \right)'$ and $\left(\frac{\partial}{\partial y} \frac{(v')^2}{2} \right)'$ in the source term is omitted since they are comparably small considering vortex sound problems. Besides, the viscous effect $\left(\frac{\partial}{\partial x} \cdot \frac{\boldsymbol{\tau}}{\bar{\rho}} \right)'$ and $\left(\frac{\partial}{\partial y} \cdot \frac{\boldsymbol{\tau}}{\bar{\rho}} \right)'$ in acoustic analysis usually assumed to be negligible. As a result, the important source term without heat source are $(\boldsymbol{\omega} v)'$ and $-(\boldsymbol{\omega} u)'$.

3. NUMERICAL METHODS

The Acoustic Perturbation Equations in the strong conservative form (Eq.1) is a set of physical conservation laws, which satisfies the requirement of a novel inexpensive numerical method - CE/SE method. It is based on a framework that ensures the flux conservation in both space and time. The method unifies the treatment to space and time dimensions, which is unique to other numerical method (7). This method is employed to solve the governing equation Eq. 1-5.

In two dimensional case, the CE/SE works on a three dimensional Euclidean space \mathbf{E}_3 with $\mathbf{X} = (x, y, t)$. The integral form of Eq. 1 without source term becomes

$$\oint_{S(V)} \mathbf{K} \cdot d\mathbf{s} = 0, \quad (6)$$

where $\mathbf{K}(\mathbf{X}) = [F(\mathbf{X}), G(\mathbf{X}), U(\mathbf{X})]$, $S(V)$ denotes the 'surface' around an arbitrary volume V in \mathbf{E}_3 , $\mathbf{K} \cdot d\mathbf{s}$ is the space-time flux passing through $S(V)$, and $d\mathbf{s} = (dx, dy, dt)$ is the normal pointing out of $S(V)$. Since Eq. 6 does not include the source term, therefore a treatment is needed to evaluate its effect and this will be

discussed later in this section. In this paper, only the concept of CE/SE method is mentioned. Readers can refer to reference (8) for the details of CE/SE method.

The definitions of conservation element (CE) and solution element (SE) are illustrated in Figure 1b and Figure 1c. The point at $(n+1/2)$ -th and n -th time level are denoted by the superscript '' and ' respectively, while no superscript denotes the point at $(n-1/2)$ -th time level. In a computational domain consists of non-overlapping triangles as shown in Figure 1a, the points A, B, C, D, E, F define the base of the conservation element (CE) which is extruded by half time step $dt/2$ to form a control volume V for flux conservation. The solution point g is the spatial centroid of ABCDEF. At time level n , CE at g is $CE(g,n)$, and the solution element (SE) at spatial location g and n -th time level is denoted by $SE(g,n)$. The adjacent $SE(a,n)$, $SE(c,n)$, and $SE(e,n)$, form the walls of $CE(g,n)$ and helps to evaluate the flux through these walls. The flux is calculated by the first order of Taylor expansions at the solution point, i.e. $\phi(\mathbf{X}) = \phi + \delta x(\phi_x) + \delta y(\phi_y) + \delta t(\phi_t)$, where $\phi(\mathbf{X}) = \mathbf{U}(\mathbf{X}), \mathbf{F}(\mathbf{X})$ or $\mathbf{G}(\mathbf{X})$, $\delta x = x - x_g$, $\delta y = y - y_g$, $\delta t = t - t^n$ and ϕ_x, ϕ_y, ϕ_t are the spatial gradients and time derivatives. From the flux conservation within $CE(g,n)$, the solution $\mathbf{U}(g)$ at the new time level $\mathbf{U}_g^{n+1/2}$ can be expressed

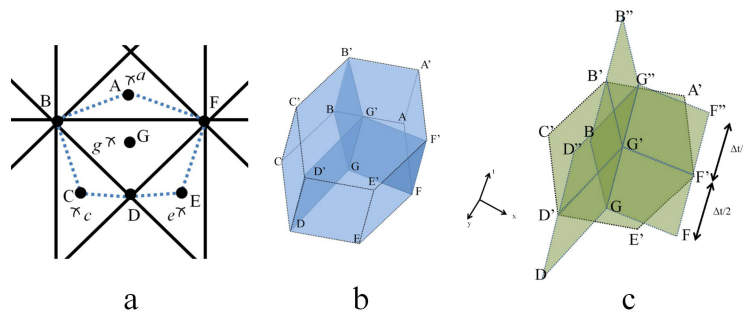


Figure 1 – Definition of CE/SE. a. CE construction; b. CE; c. SE

as the function of the solutions of $\mathbf{U}(a), \mathbf{U}(c), \mathbf{U}(e)$ at the time level n . Since all the solutions of the time level n are known, the solution at the new time level $n + 1/2$ can be determined.

The source term \mathbf{Q} is treated as a volume source in the $CE(g,n)$ i.e. the appropriate solution should be $\hat{\mathbf{U}}_g^{n+1/2} = \mathbf{U}_g^{n+1/2} + \int \mathbf{Q} dt$. This method is only applicable if \mathbf{Q} is independent of the solution vector. Otherwise, iteration method is required to evaluate the solution. Though the solution vector involves total quantity which consists of unknown fluctuating components having dependency on solution vector, they are very small compare to time averaged component. Thus, they are negligible which makes this implementation of the source term plausible. The new spatial gradients of the solution vector $(\hat{\mathbf{U}}_g^{n+1/2})_x$ and $(\hat{\mathbf{U}}_g^{n+1/2})_y$ will then be updated having evaluated the $n+1/2$ -th time level solution $\hat{\mathbf{U}}_g^{n+1/2}$.

4. TIME-DOMAIN IMPEDANCE BOUNDARY CONDITION

In CE/SE method, all boundary conditions are implemented by using ghost cell approach, appropriate values of pressure and velocity are required to assign to the ghost cell across the boundary. Therefore, the acoustic pressure gradient $\frac{\partial p'}{\partial n}$ across the boundary condition is required for the pressure specification.

The implementation of the time domain impedance boundary condition (TDIBC) in CE/SE method follows the impedance boundary condition proposed by Tam and Auriault (9), which is based on the three-parameter model. First of all, the acoustic impedance is defined as $Z = v'_n/p'$, $Z = R - iX$ where v'_n is the acoustic velocity normal to the impedance surface. The acoustic resistance R is nearly a positive constant, i.e. $R = R_0$, while the acoustic reactance X is frequency dependent and can be decomposed to a positive reactance X_1 and negative reactance X_{-1} , i.e.

$$\frac{X}{\bar{\rho} \bar{c}} = \frac{X_{-1}}{\omega} + X_1 \omega, \tag{7}$$

where $\bar{\rho}, \bar{c}$ are the reference density and the reference acoustic speed, and ω is the angular frequency. The three-parameter broadband model governing the rate of change of the acoustic pressure at the impedance boundary is

$$\frac{\partial p'}{\partial t} = R_0 \frac{\partial v'_n}{\partial t} - X_{-1} v'_n + X_1 \frac{\partial^2 v'_n}{\partial t^2}. \tag{8}$$

Define a new auxiliary variable $q(\xi, t) = \frac{\partial v'_n}{\partial t}$ at the impedance boundary $n = 0$, Eq. 8 can be rewritten after

eliminating $\frac{\partial p'}{\partial t}$ by the perturbed equations Eq. 1-5,

$$\frac{\partial q}{\partial t} = -\frac{1}{X_1} \left[R_0 q - X_{-1} v'_n + \bar{c}^2 \frac{\partial}{\partial n} \left(\bar{\rho} v'_n + \bar{v}_n \frac{p'}{c^2} \right) + \bar{c}^2 \frac{\partial}{\partial \xi} \left(\bar{\rho} v'_\xi + \bar{v}_\xi \frac{p'}{c^2} \right) \right], \quad (9)$$

where ξ is the tangential vector to the impedance surface normal vector. Acoustic pressure relationship across the impedance boundary can be obtained from the conservation of momentum in normal direction. Neglecting all the small nonlinear fluctuating products, i.e.

$$\frac{\partial p'}{\partial n} = -\bar{c}^2 q. \quad (10)$$

The acoustic pressure in the ghost cell can be obtained by the pressure gradient, and then the ghost cell velocity can be obtained from the auxiliary variable and its derivative.

5. RESULT AND DISCUSSION

In the investigation of a silencer performance, it is important to correctly capture the generation of noise by the unsteady flow, its propagation within the confined duct as well as its response after impinging on the acoustic impedance walls. Therefore, it is very important to assess the capability of the new calculation method in capturing all these physics. Three benchmark problems are chosen for this purpose and their calculation results are discussed below.

5.1 Acoustic Generation by Co-rotating Vortices

The acoustic generation from a pair of co-rotating vortices is calculated to assess the capability of capturing acoustic generation and propagation by an unsteady flow. In fluid dynamics, the flow of a co-rotating vortex pair is a simplified model of common vortical flows. Spiral acoustic pattern is generated from this spinning vortex pair (10, 11), due to their periodic co-rotating motion. In the present calculation, the two vortices with the same circulation Γ are co-rotating in a path with radius r_0 as illustrated in Figure 2a. To compute the acoustic field, the incompressible velocity and pressure field data are required as input of the acoustic solver and they are given by analytical solution. The incompressible velocity field is expressed as $U - iV = \frac{\Gamma}{i\pi} \frac{z}{z^2 - b^2}$, $P = P_a + \rho_a \frac{\Gamma \omega}{\pi} \Re \left(\frac{b^2}{z^2 - b^2} \right) - \frac{1}{2} \rho_a (U^2 + V^2)$, where the angular speed $\omega = \Gamma / (4\pi r_0^2)$, $z = x + iy = r e^{i\theta}$ and $b = r_0 e^{i\omega t}$ are the spatial location and the location of the vortices respectively. Non-reflecting boundary condition is applied to the boundaries in the computational domain to ensure no unwanted reflection affecting the solution. The analytical solution on the acoustic generation from the spinning vortex pair is obtained by

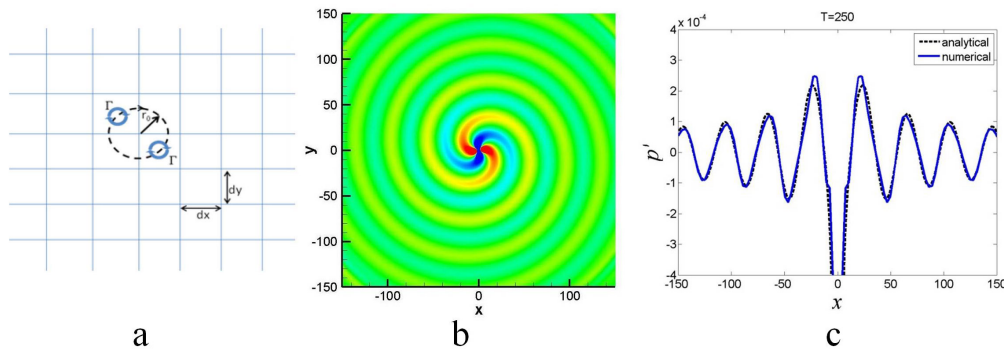


Figure 2 – a. Illustration of the problem; b. Generated acoustic pressure at $T=250$; c. Comparison of acoustic pressure along $y=0$

Kaltenbacher (12) is

$$p' = \frac{\rho_a \Gamma^4}{64\pi^3 r_0^4 c_a^2} (J_2(kr) \cos(2(\omega t - \theta)) - Y_2(kr) \sin(2(\omega t - \theta))) \quad (11)$$

where $k = 2\omega/c_a$, $J_2(kr)$ and $Y_2(kr)$ are second-order Bessel functions of the first and second kind. The dimensionless circulation is set to $\Gamma = 1$ and $r_0 = 1$, corresponding to the analytical acoustic wave length

$\lambda = 39$.

The simulated acoustic field generation is plotted in Figure 2b, which shows that the generated acoustic wave radiates as a double spiral pattern. The calculated wave length is 39, which is the same as the analytical solution. Furthermore, the acoustic pressure data at the horizontal centreline of the numerical domain and is compared with the analytical result in figure 2c. It shows a good agreement between the analytical and numerical results in terms of wave length, amplitude and the propagation decay rate. This calculation demonstrates the present calculation method is capable to capture the acoustic generation and propagation from vortical source.

5.2 Reflection of Acoustic Pulse in Impedance Tube

Calculation of an acoustic pulse reflection in a normal incidence impedance tube (Figure 3) is chosen to assess the capability of the TDIBC behavior without mean flow under normal incidence using the present calculation method. The impedance tube is constructed as same as that adopted by Tam and Auriault (9) with dimensionless length 150 and the duct width of 10. The impedance wall is defined as a broadband impedance boundary with normalized impedance $R=0.18$, $X_{-1}=-0.47567$ and $X_1=2.09236$ (9, 13). An initial harmonic-Gaussian pulse within the tube is located at $x=-83.333$ and is given by,

$$u' = 0, p' = 10^{-4} e^{-0.00444(x+83.333)^2} \cos(0.00444(x + 83.333)). \quad (12)$$

Non-reflecting boundary condition is applied to the upstream of the acoustic pulse. Slip wall boundary is also

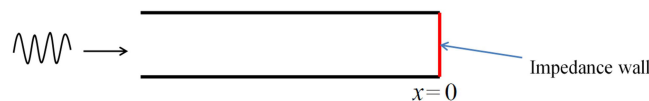


Figure 3 – Normal incidence impedance tube

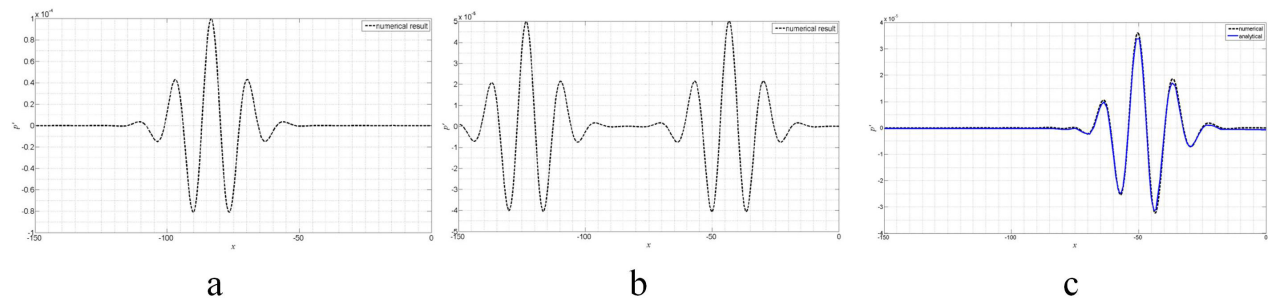


Figure 4 – Acoustic pressure along $y=0$. a. $t=0$; b. $t=40$; c. $t=140.1$;

applied to the top and the bottom wall of the tube and finally TDIBC is applied to the impedance wall.

After calculation starts, the pulse separates into two halves (Figure 4a). One travels to the left, while the other half moves to the right (Figure 4b). It impinges on the impedance wall and reflects from it. The reflected pulse at $t=140.1$ is shown in Figure 4c. The result shows that the amplitude of the reflected pulse is weaker than that of the incident pulse by 20%. Besides, the leading peak and the trailing peak are no longer symmetric with respect to the highest peak. The calculated result (dotted line) shows a good agreement with the analytical solution (solid line), this implies that the TDIBC with this acoustic solver can capture the absorption and reflection behavior of impedance wall correctly.

5.3 Acoustic Propagation in Grazing Incidence Tube

The last problem chosen for calculation is the Grazing Incidence Tube (GIT) experiment carried out by NASA (14) which shows the behavior of an acoustic wave grazing incidences to TDIBC in the presence and absence of flow. This problem has been used as a benchmark validation on the various computational aeroacoustic solvers involving TDIBC (Ozyoruk and Long (15), Zheng and Zhuang (16), and Li et al. (17)). The GIT experiment configuration is shown in Figure 5. A few settings on flow speed and frequency are picked for calculation, 0.5kHz and 2.5kHz are introduced to the GIT under flow with average Mach number $M = 0$ and 1.5kHz is introduced to the tube under flow with $M = 0.255$. In the calculation, non-reflecting boundary condition is applied to both upstream and downstream exits representing the anechoic termination, slip wall boundary conditions is applied to the tube while TDIBC is applied in the impedance wall.

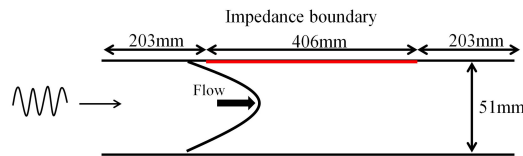


Figure 5 – Configuration of NASA GIT

$f(\text{kHz})$	$M = 0$		$M = 0.225$	
	R	X	R	X
0.5	0.51	-1.68	0.57	-1.13
1	0.46	0.00	0.27	0.10
1.5	1.02	1.30	1.26	1.26
2	4.05	0.62	6.43	-0.23
2.5	1.54	-1.60	1.02	-1.46
3	0.70	-0.29	0.73	-0.18

Table 1 – measured impedance from NAGA GIT experiment

The calculated sound pressure level (SPL) distribution on the wall opposite to the impedance wall is compared with the experimental result. Figure 6 shows the SPL distribution near the opposite wall to the TDIBC under 500Hz and 2500Hz excitation respectively. In Figure 6a there is an 1dB difference from $x = 0.2$ to $x = 0.65$, i.e. within the liner section. The result of zero mean flow with 2500Hz excitation agrees with the experimental result very well. Generally, the numerical result matches with the experimental result in terms of amplitude and the decay rate.

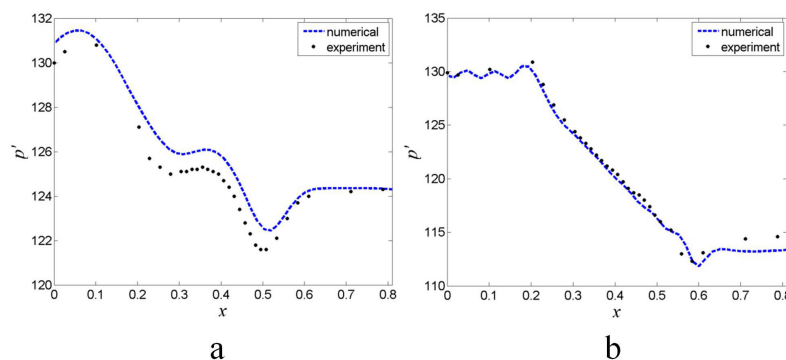


Figure 6 – SPL distribution under zero mean flow. a. 500Hz; b. 2500Hz

Figure 7 shows the result of glazing impedance tube under flow with $M = 0.255$. A parabolic velocity profile is introduced into the tube. The result matches with the general trends of the experimental result. This shows the present calculation method is capable to calculate the grazing incidence acoustic wave on impedance surface correctly.

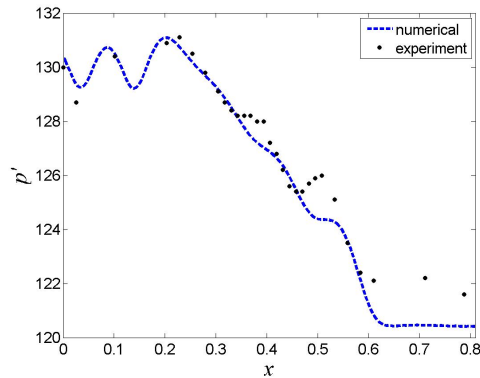


Figure 7 – SPL distribution under 0.255 Mach number mean flow and 1500Hz excitation

6. CONCLUSIONS

In this paper, a method of calculating the flow duct noise problem is presented, which solves the Acoustic Perturbation Equations by using the CE/SE method and the time-domain impedance boundary is implemented. In order to assess the capability of this method on capturing acoustic generation, propagation, and the impedance behavior with and without flow, three benchmark problems have been chosen to be calculated using the current calculation method. The three benchmark problems are acoustic generation by co-rotating vortices, reflection of acoustic pulse in impedance tube and acoustic propagation in grazing incidence tube. All the results show good agreement to the analytical or experimental results which implies that this calculation method is capable to predict the acoustic behavior in different flow duct problems.

ACKNOWLEDGEMENTS

The authors gratefully acknowledge the supports given by the Research Grants Council of Hong Kong SAR Government under Grant Nos. PolyU 5119/11E.

REFERENCES

1. Hardin JC, Pope DS. An acoustic/viscous splitting technique for computational aeroacoustics. *Theoretical and Computational Fluid Dynamics*. 1994 Oct;6(5-6):323–340.
2. Bogey C, Bailly C, Juvé D. Computation of flow noise using source terms in linearized Euler's equations. *AIAA journal*. 2002;40(2).
3. Ewert R, Schröder W. Acoustic perturbation equations based on flow decomposition via source filtering. *Journal of Computational Physics*. 2003 Jul;188(2):365–398.
4. Ma Z, Zhang X. Numerical Investigation of Broadband Slat Noise Attenuation with Acoustic Liner Treatment. *AIAA Journal*. 2009 Dec;47(12):2812–2820.
5. Shen W, Sørensen J. Comment on the aeroacoustic formulation of Hardin and Pope. *AIAA Journal*. 1999;37(1):1–3.
6. Seo JH, Moon Y. Perturbed Compressible Equations for Aeroacoustic Noise Prediction at Low Mach Numbers. *AIAA Journal*. 2005 Aug;43(8):1716–1724.
7. Wang XY, Chang SC. A 2D Non-splitting Unstructured Triangular mesh Euler Solver Based on the Space-Time Conservation Element and Solution Element Method. *Computational Fluid Dynamics Journal*. 1999;8(2):309–325.
8. Lam GCY, Leung RCK, Seid KH, Tang SK. Validation of CE/SE Scheme in Low Mach Number Direct Aeroacoustic Simulation. *International Journal of Nonlinear Sciences and Numerical Simulation*. 2014 Jan;p. 1–16.
9. Tam CKW, Auriault L. Time-Domain Impedance Boundary Conditions for Computational Aeroacoustics. *AIAA Journal*. 1996;34(5):917–923.
10. Powell A. Theory of vortex sound. *The journal of the acoustical society of America*. 1964;36(1):177–195.

11. Müller EA, Obermeier F. The spinning vortices as a source of sound. AGARD CP-22. 1967;p. 1–7.
12. Kaltenbacher M, Escobar M, Becker S, Ali I. Numerical simulation of flow-induced noise using LES/SAS and Lighthill's acoustic analogy. *International Journal for Numerical Methods in Fluids*. 2009;63:1103–1122.
13. Mottsinger RE, Kraft RE. Design and performance of duct acoustic treatment. In: NASA. Langley Research Center, *Aeroacoustics of Flight Vehicles: Theory and Practice*. Volume 2: Noise Control; 1991. p. 165–206.
14. Jones M, Watson W, Parrott T. Benchmark Data for Evaluation of Aeroacoustic Propagation Codes with Grazing Flow. *AIAA Paper*. 2005 May;p. 2005–2583.
15. Ozyoruk Y, Long LN. Time-Domain Calculation of Sound Propagation in Lined Ducts with Sheared Flows. *AIAA Journal*. 2000 May;38(5):768–773.
16. Zheng S, Zhuang M. Verification and Validation of Time-Domain Impedance. *AIAA Journal*. 2005;43(2).
17. Li XD, Richter C, Thiele F. Time-domain impedance boundary conditions for surfaces with subsonic mean flows. *The Journal of the Acoustical Society of America*. 2006;119(5):2665.